

Analyst

Accepted Manuscript



This is an *Accepted Manuscript*, which has been through the Royal Society of Chemistry peer review process and has been accepted for publication.

Accepted Manuscripts are published online shortly after acceptance, before technical editing, formatting and proof reading. Using this free service, authors can make their results available to the community, in citable form, before we publish the edited article. We will replace this *Accepted Manuscript* with the edited and formatted *Advance Article* as soon as it is available.

You can find more information about *Accepted Manuscripts* in the [Information for Authors](#).

Please note that technical editing may introduce minor changes to the text and/or graphics, which may alter content. The journal's standard [Terms & Conditions](#) and the [Ethical guidelines](#) still apply. In no event shall the Royal Society of Chemistry be held responsible for any errors or omissions in this *Accepted Manuscript* or any consequences arising from the use of any information it contains.

1
2
3
4 **1 An electrochemical impedimetric sensor based on**
5
6 **2 biomimetic eletrospun nanofibers for formaldehyde**
7
8

9
10 3 Hong Dai^{a*}, Lingshan Gong^a, Guifang Xu^a, Xiuhua Li^a, Shupeizhang^a, Yanyu Lin^{a,b},

11
12 4 Baoshan Zeng^a, Caiping Yang^b, Guonan Chen^{b*}
13

14
15 5 a College of Chemistry and Chemical Engineering, Fujian Normal University, Fuzhou, Fujian,

16
17 6 350108,P.R. China
18

19
20 7 b Ministry of Education Key Laboratory of Analysis and Detection for Food Safety, and

21
22 8 Department of Chemistry, Fuzhou University, Fuzhou, Fujian 350002, P.R. China
23

24
25 9

26
27
28 10 Corresponding author

29
30 11 Fax: (+86)-591-22866135;

31
32 12 E-mail: dhong@fjnu.edu.cn (H. Dai)

33
34 13 gnchen@fzu.edu.cn (G. Chen);
35
36

37
38 14

39
40 15
41
42
43
44
45
46
47
48
49
50
51
52
53
54
55
56
57
58
59
60

1
2
3
4 **Abstract**
5

6 Herein, simple molecular recognition sites for formaldehyde were designed on
7
8 electrospun polymer nanofibers. In order to improve the conductivity of the
9
10 electrospun polymer nanofibers, carbon nanotubes were introduced into the resultant
11
12 nanofibers. By employing these functionalized nanocomposite fibers to fabricate the
13
14 biomimetic sensor platform, obvious change caused by recognition between
15
16 recognition sites and formaldehyde molecules was monitored through
17
18 electrochemical impedance spectroscopy (EIS). The experiment conditions were
19
20 optimized and then the quantitative method for formaldehyde in low concentration
21
22 was established. The relative results demonstrated the sensor based on biomimetic
23
24 recognition nanofibers displays an excellent recognition capacity to formaldehyde.
25
26 The linear response range of the sensor was between $1 \times 10^{-6} \text{ mol} \cdot \text{L}^{-1}$ and 1×10^{-2}
27
28 $\text{mol} \cdot \text{L}^{-1}$, with the detection limit of $8 \times 10^{-7} \text{ mol} \cdot \text{L}^{-1}$. The presented research provided
29
30 a fast, feasible and sensitive method for formaldehyde with good anti-interference
31
32 capabilities and good stability, which could meet the practical requirement for
33
34 formaldehyde assay.
35
36
37
38
39
40
41
42
43

44 **Key words:** electrochemical impedance spectroscopy, biomimetic recognition,
45
46 formaldehyde, electrospun nanofibers, poly(methacryloylhydrazide)
47
48
49
50
51
52
53
54
55
56
57
58
59
60

1 **Introduction**

2 Highly selective recognition is one of biological functions in the natural system,
3 including immune reaction and enzymatic processes. However, there were inherent
4 limitations with respect to expensive, limited life and stability¹. Therefore, to
5 overcome these limitations, in recent years, material scientists and engineers drew the
6 inspiration from biological systems had attracted much focus to design economically
7 and functionally efficient biomimetic receptors allowing for substrate binding
8 characteristics similar to natural systems^{1,2}. In the biomimetic recognition systems
9 included an indicator molecule which carried a suitable binding site and the
10 analyte-receptor types involved various interactional methods, such as hydrophobic
11 interactions, affinity-based ones, hydrogen bonds, polar interactions and covalent
12 interactions². C=N bond formed from condensation of amino and carboxyl has been a
13 superior and attracted lots of attention as the relation of imines in realms of
14 chemistry and biology³. This reaction is widely distributed in nature and possesses
15 significance in many pharmacological activities, such as transformations of amino
16 acid and the cofactor, pyridoxal (vitamin B₆)^{4,5}. Biomimetic recognition materials
17 with pre-designed recognition sites exhibit a quite promising application and have
18 many obvious advantages in sensors field, including low cost, simplicity, and
19 reliability⁶⁻¹¹. For instance, the traditional molecule imprinted technology was widely
20 used as the biomimetic recognition, due to the complementarities in recognition sites
21 and shape, molecule imprinted polymers work as synthetic antibodies toward target
22 molecules^{6,9}, including various metal ions¹², organic molecules¹³ or bioorganic

1 molecules¹⁴. Herein, molecule imprinted polymers could be used to establish mimic
2 biosensor with artificial and controllable recognition capability, resulting from its rich
3 artificial recognition elements and highly sensitive sensing effect. However, the
4 analytical properties of this kind sensor mainly depend on the quantity of effective
5 recognition sites of the molecularly imprinted polymer film⁹. The main issues
6 restricting biomimetic recognition technology are its relatively narrow response
7 kinetic range, bulk monolith and large template size limitations¹⁵. By coating a quite
8 thin polymer film on a support, it could permit target molecules access easily,
9 however, the binding capacity in the same area of designed device decreases. So the
10 sensitivity and the linear response of the mimic biosensor structured by this strategy
11 always cannot achieve desired effect¹⁵⁻¹⁸. With respect to the improvement of mimic
12 biological functions, nanostructure materials with abundant recognition sites are
13 dramatically appealing. Due to higher specific surface area, nanostructures for
14 biomimetic recognition are believed to have better performance than the larger scales.
15 As well known, preparation of sensing materials in form of nanostructures may
16 significantly improve the performances in the sensing devices and open the door to
17 new types of applications. Electrospinning, which is an interesting and
18 well-characterized physical phenomenon, opens new economically viable possibilities
19 to produce nanofibers (NFs) with high-quality and low cost. Electrospun nanofibers
20 are featured with large specific surface area, high porosity, which made them highly
21 attractive to different applications in filtration, drug delivery platform, tissue
22 engineering and so on. However, till now, there were rare reports about employing

1 electrospun nanofibers, which can enhance the recognition sites on the surface of the
2 electrospinning nanofibers, as the sensing element to fabricate the biomimetic sensor.
3 Compared with traditional biomimetic materials, the prepared biomimetic recognition
4 nanofibers exhibited superior features such as faster binding kinetics and higher target
5 binding capacity. Moreover, to improve functions of nanofibers, electrospinning
6 technique has also been used to create various kinds of fibrous nanomaterials by
7 adulterating other functional materials^{19,20}, such as nanoparticle, biomolecules and
8 carbon nanotubes into the polymer nanofibers. Carbon nanotubes (CNTs) consist of
9 seamless cylindrical graphitic sheets. As a sort of carbon nanomaterials with
10 intriguing structures and unique preproperties²¹, such as large specific surface area and
11 capacitance, good conductivity and fast electron transfer rate, CNTs attracted
12 intensive attention in lots of fields²² for example composite materials, nanoelectronic
13 devices. Compared to polymer/metal nanoparticles and other composite materials, the
14 high aspect ratio of the carbon nanotube is beneficial to improve material percolation
15 conductivity properties²³. In our study, we proposed the new and facile
16 electrospinning technology to create CNTs hybrid nanofibers to improve the
17 biomimetic sensor performance.

18 Formaldehyde, a simple organic compound, is an important chemical found in many
19 consumer products and works as a sterilising agent²⁴. Formaldehyde has a great
20 impact on human health, because of its potentially carcinogenic and mutagenic
21 properties and its capability of forming intermediate and stable species of toxic and
22 phototoxic radicals^{13,25}. Thus, various quantitative methods for formaldehyde including

1
2
3
4 1 gas chromatogram, electrochemistry, chemiluminescence and piezoelectric sensor etc
5
6 2 have been established²⁵⁻²⁸. Electrochemical impedance spectroscopy is a sensitive
7
8
9 3 indicator of a variety of chemical and physical properties. Thus, impedimetric sensor,
10
11 4 which owns the features associated with electrochemical approaches, namely the
12
13 5 ability to be miniaturized, highly sensitivity, low cost of electrode mass production
14
15 6 and cost effective instrumentation, etc, have attracted much attention, for example Liu
16
17 7 et al reported room temperature impedance spectroscopy-based sensing of
18
19 8 formaldehyde with porous TiO₂ under ultraviolet illumination²⁹ and others'
20
21 9 investigations^{30,31}. However, to the best of our knowledge, limited impedimetric
22
23
24 10 sensors have been developed to detect formaldehyde. Herein, the electrospun
25
26 11 nanofibers for formaldehyde was designed and firstly employed as the bio-recognition
27
28 12 element to fabricate biomimetic sensor based on electrochemical impedance
29
30 13 spectroscopy. Benefited from the unique properties of electrospun biomimetic
31
32 14 recogniton nanofibers, the impedimetric sensor prepared by this material exhibited
33
34 15 obvious sensitivity, stability and selectivity towards formaldehyde. On this basis, this
35
36 16 biomimetic impedimetric sensor based on biomimetic nanofibers was proposed for
37
38 17 preparing new artificial biosensor with molecular recognition properties, which could
39
40 18 be extended in environmental monitoring, food inspection and medical diagnosis and
41
42 19 so on.
43
44
45
46
47
48
49
50

51 **Experimental Section**

52 **Chemicals**

53
54
55
56
57 22 Ploymethylnmethacrylate (PMMA) was obtained from Sigma (St. Louis, MO, USA)
58
59
60

1 and used without further purification. Carbon nanotubes were purchased from
2 Nanport. Co. Ltd. (Shenzhen, China). Other reagents were of analytical reagents. The
3 water used for the preparation of the solution was purified by a Water Purifier (China)
4 purification system.

5 **Instruments and measurements**

6 Electrochemical impedance spectroscopy (EIS) and cyclic voltammetry (CV) were
7 performed with a CHI 760 electrochemical analyzer (Shanghai Chenghua Instrument
8 Co., China). All electrochemical procedures were carried out with a three-electrode
9 system comprising a platinum wire auxiliary electrode, Ag/AgCl reference electrode
10 (sat. KCl) and a glassy carbon electrode (GCE, $\phi=3$ mm) which served as the working
11 electrode. Fourier Transform Infrared (FTIR) microscope was measured on a Nicolet
12 6700 FTIR spectrometer (Nicolet, USA).

13 **Synthesis of ploy-methacryloylhydrazide (PMAH)**

14 Ploy-methacryloylhydrazide was synthesized according to the previous report³².
15 Briefly, PMMA was dissolved in dichloromethane. The reaction was carried out in
16 1:1 mixture of PMMA and hydrazine hydrate (n/n) with stirring at room temperature.
17 The product was extracted with ethanol. At last, a white solid matter, PMAH, was
18 obtained for the subsequent use.

19 **Electrospinning**

20 The homogeneous solution was prepared with dissolving 8 wt% PMAH into
21 N,N-Dimethylformamide under magnetic stirring for 8 h. Then 0.5 wt% CNTs was

1 added into this solution, followed by vigorous stirring at room temperature for 16 h.
2
3 PMAH/CNTs-NFs were fabricated by electrospinning utilizing a metallic needle to a
4
5
6
7
8
9
10
11
12
13
14
15
16
17
18
19
20
21
22
23
24
25
26
27
28
29
30
31
32
33
34
35
36
37
38
39
40
41
42
43
44
45
46
47
48
49
50
51
52
53
54
55
56
57
58
59
60

6 **Preparation of modified glassy carbon electrode**

7 Before modification, the bare glassy carbon electrode (GCE, 3 mm in diameter) was
8
9
10
11
12
13
14
15
16
17
18
19
20
21
22
23
24
25
26
27
28
29
30
31
32
33
34
35
36
37
38
39
40
41
42
43
44
45
46
47
48
49
50
51
52
53
54
55
56
57
58
59
60

19 **Results and Discussion**

20 **Principle of the biomimetic sensor**

21 The biomimetic sensor was fabricated, as it shown in Scheme 1. Firstly, PMAH,

1 which owns the electrospun property, was synthesized. Then, in order to improve the
2 electrochemical activity of the fabricated nanofibers, CNTs were introduced into the
3 electrospun solution to fabricate biomimetic recognition elements. Secondly, the
4 fabricated nanofibers with biomimetic function were immobilized onto the sensing
5 matrix. Due to the interaction between formaldehyde and the fabricated PMAH
6 electrospun nanofibers, which is nucleophilic addition reaction of carbonyl and amino,
7 and the result produce is very unstable and easily lose H₂O then formed imine (Schiff
8 base)^{32,33}, great change of electron transfer resistance at the biomimetic sensor was
9 observed. Then, the biomimetic sensor for formaldehyde based on electrochemical
10 impedance spectroscopy was obtained.

11 **Characterization of PMAH**

12 Figure 1A shows the scanning electron microscope (SEM) image which exhibits the
13 nanofibers possess average diameter and are initially produced without large bead,
14 and the CNTs do not appear on the surface of the nanofibers. Therefore, it presents
15 that the appropriate tension of the complex for electrospinning. Figure 1B displays the
16 transmission electron microscope (TEM) image of the nanofibers, it can be obviously
17 found that the CNTs in the nanofibers are well dispersed and the end of CNTs
18 actually range in sequence at the surface of the nanofibers due to the effect of electric
19 field, which can well avoid the physics absorption of the CNTs to target molecule. It's
20 well known the end of CNTs own highly electrochemical catalysis. Hence, the unique
21 construction of this electrospun material possibly owns some advantages in
22 establishing CNTs assisted biomimetic recognition sensor. Figure 1C shows the

1 typical FTIR spectrums of PMAH (a) and PMMA (b). Some characteristic absorption
2 bands of PMMA (Figure 1b), such as the C-H asymmetric and symmetric stretching
3 frequencies (2954 cm^{-1}), CH_2 bending vibrations (1435 cm^{-1}), and a broad intense
4 band due to the stretching vibrations of the O-H groups from intercalated water were
5 observed¹⁰. Comparing with Figure 1b, there was an evident stretching peak presented
6 in 1244 cm^{-1} in Figure 1a, owing to the stretching characteristic peak of C-N¹⁰. It
7 could strongly proved ploy-methacryloylhydrazide was successfully synthesized.

8 **Electrochemical behavior of electrospun nanofibers modified electrodes**

9 Different cyclic voltammograms of various modified electrodes in $5\text{ mmol}\cdot\text{L}^{-1}$
10 $\text{Fe}(\text{CN})_6^{3-}$ solution containing $0.1\text{ mol}\cdot\text{L}^{-1}$ KCl are shown in Figure 2A. A classical
11 pair of redox peaks is obtained at GCE. Due to the existence of insulative PMAH
12 nanofibers on sensing interface, it works as a barrier to arrest the electron transfer
13 between electrode surface and $\text{Fe}(\text{CN})_6^{3-/4-}$. So the redox peak response at
14 PMAH-NFs/GCE is obviously depressed. After CNTs are doped into the nanofibers,
15 the current of redox peaks are recovered, which indicates that the good conductivity
16 and high surface area of CNTs can improve the electrochemical activity of
17 electrospun nanofibers^{15,35}. With immersing in $0.01\text{ mol}\cdot\text{L}^{-1}$ formaldehyde solution
18 for 60 s, the redox peaks at the PMAH/CNTs-NFs/GCE is a slightly smaller than
19 without, resulting from the molecular recognition sites of the PMAH/CNTs-NFs taken
20 up by formaldehyde, then leading to the obstruction of the electron transfer between
21 sensing interface and electrochemical probe.
22 Electrochemical impedance was also employed to characterize various modified

1
2
3
4 1 electrodes. In electrochemical impedance measurement, the semicircle obtained at
5
6 2 high modulation frequency describes the Faradic electron-transfer process at the
7
8 3 electrode interface, whereas the straight region obtained at the lower modulation
9
10 4 frequency contains information about the diffusion-limited transport of the redox
11
12 5 species in the electrolyte to the electrode interface. Figure 2B shows the
13
14 6 electrochemical impedance spectra (EIS) of various electrodes in $5 \text{ mmol}\cdot\text{L}^{-1}$
15
16 7 $[\text{Fe}(\text{CN})_6]^{3-/4-}$ containing $0.1 \text{ mol}\cdot\text{L}^{-1}$ KCl. It can be seen that a well defined
17
18 8 semi-circle at higher frequencies is obtained at these electrodes. When PMAH
19
20 9 nanofibers was modified on the surface of GCE, the impedance value was
21
22 10 substantially increased and it was nearly forty thousand times greater than that case at
23
24 11 GCE, suggesting that PMAH nanofibers blocked the charge migration between
25
26 12 electrode surface and redox probe. However, when CNTs were doped into the
27
28 13 nanofibers and were dropped onto GCE, the electron transfer resistance was
29
30 14 effectively reduced. The present of CNTs, which have many high catalysis activity
31
32 15 sites, could accelerate the charge migration. After PMAH/CNT-NFs/GCE was
33
34 16 immersed in $0.01 \text{ mol}\cdot\text{L}^{-1}$ formaldehyde solution for 60 s, the impedance value
35
36 17 increased, which was due to the molecular recognition sites of the PMAH/CNT-NFs
37
38 18 plugged by formaldehyde, and led to the block effect of the charge migration between
39
40 19 electrode surface and $\text{Fe}(\text{CN})_6^{3-/4-}$. This phenomenon was similar to the performance
41
42 20 of the cyclic voltammograms above.
43
44 21 Figure 3A shows Nyquist diagrams of electrochemical impedance spectra of various
45
46 22 modified electrodes before and after recognizing formaldehyde. It can be seen that all
47
48
49
50
51
52
53
54
55
56
57
58
59
60

1 these electrodes obtained a well defined semi-circle at higher frequencies. The
2 impedance value of PMAH-NFs/GCE incubated with $0.01 \text{ mol}\cdot\text{L}^{-1}$ formaldehyde
3 solution for 60 s was remarkably higher than other electrodes. And the
4 PMAH-NFs/GCE had a high impedance value. Whereas, when carbon nanotubes
5 were doped into producing the electrospun nanofibers, the impedance value was
6 remarkably decreased, due to the good conductivity of CNTs.

7 In order to take into account the resistance contribution from the specific interaction
8 between formaldehyde and the sensing interface and improve the signal-to-noise and
9 sensitivity, the changes in resistance were calculated according to the following
10 expressions:

$$\frac{\Delta R}{R} = \frac{R^* - R}{R}$$

11 where R^* and R represented the value of the electron transfer resistance of the
12 modified electrode before and after the incubation with certain concentration of
13 formaldehyde. The value of $\Delta R/R$ at PMAH/CNT-NFs/GCE was much higher than
14 that case at PMAH-NFs/GCE, indicating carbon nanotubes doped into the nanofibers
15 could improve the sensitivity of this biomimetic sensor.

16 As a kind of nanomaterials with inherent structures and unique properties, such as
17 large specific surface area and capability, good conductivity and fast electron transfer
18 rate, CNTs attracted intensive attention in lots of fields for example composite
19 materials, nanoelectronic devices. Here, CNTs were used as functional material to
20 improve the properties of electrospinning fibers. The EIS of PMAH and CNTs formed
21 composite film modified electrode (PMAH/CNT/GCE) and the nanofibers containing
22

1 PMAH and CNTs (PMAH/CNT-NFs/GCE) before and after incubating with 0.01
2 mol·L⁻¹ formaldehyde solution for 60 s were shown in Figure 3B. Compared curve a
3 and b in Figure 3B, although these two modified electrodes had the same weight of
4 CNTs and PMAH in the modified film, the EIS of these modified electrodes were
5 apparently different. Attributing to the unique nanofiber construction of CNTs and
6 PMAH formed composite, the smaller electron transfer resistance at these nanofibers
7 modified electrode was observed. After incubating with 0.01 mol·L⁻¹ formaldehyde
8 solution for 60 s, the increased electron transfer resistance could be observed at both
9 modified electrodes, indicating the ability of molecular recognition for formaldehyde
10 at the sensing interface. It should be noticed that the larger increase of electron
11 transfer resistance change is obtained at the nanofibers modified electrode, which
12 demonstrated that the composite nanofibers own more molecular recognition sites and
13 larger surface area.

14 **Molecular Recognition of the electrospun composite nanofibers**

15 Figure 4A shows that the impedance value of the PMMA-NFs/GCE is almost equate
16 to that case at the PMMA-NFs/GCE electrode after incubating with 0.01 mol·L⁻¹
17 formaldehyde solution for 60 s, indicating that PMMA which is usual molecule
18 imprinted polymer^{32,36,37}, does not have specific recognition sites and obvious
19 adsorption toward formaldehyde.

20 The electrochemical impedance response of the CNTs functionalized PMAH
21 electrospun nanofibers modified electrode was expected to be affected by the amount
22 of CNTs. As it depicted in Figure 4B, with the increased amount of CNTs in

1 fabricated nanofibers, an obviously decreased trend in electron transfer resistance was
2 found. However, the further increased amount of CNTs in nanofibers did not
3 remarkably depress the electron transfer resistance. Furthermore, the more CNTs
4 would lead to the decrease of recognition sites on the nanofibers and the unwanted
5 non-specificity adsorption. Considering the relationship between the value of $\Delta R/R$
6 and the amount of CNTs in the electrospun nanofibers, it was found that the
7 introduction of CNTs into electrospun nanofibers could improve the molecular
8 recognition effect; however, too much amount of CNTs would result in the poor
9 recognition effect. Therefore, from the aspect of improving the analytical properties,
10 the proper introduction of CNTs into the nanofibers was essential.

11 **Optimum experiment conditions**

12 The EIS of the modified electrode for certain concentration of formaldehyde was
13 expected to be affected by the amount of the CNTs and PMAH formed composite
14 nanofibers, which could be controlled easily. As shown in Figure 4C, the value of
15 $\Delta R/R$ of this sensor was increased with increasing of PMAH/CNTs-NFs
16 concentration from 1 mg/ml to 2 mg/ml. However, when the concentration was
17 beyond 2 mg/ml, the value decreased, resulting from the imprinted nanofibers
18 aggregated together and became thick membrane, then leading to slow diffusion of
19 formaldehyde to the recognition sites⁸.

20 It is well known that the preconcentration step was typically a simple and effective
21 way for enhancing the sensitivity of the imprinted sensor. In order to determine the
22 optimum operation time for formaldehyde detection, the relative experiment was

1 carried out. As it demonstrated in Figure 4D, with increasing of the preconcentration
2 time, the value of the impedance was increased, resulting from formaldehyde took up
3 the molecular recognition sites to hinder the charge migration between electrode
4 surface and $\text{Fe}(\text{CN})_6^{3-/4-}$. However, when the preconcentration time was over 60 s, the
5 responses was nearly unchanged, indicating that nearly all of the recognition sites was
6 taken up. Therefore, in order to obtain the strong electrochemical response, the
7 optimized preconcentration time was 60 s.

8 **Analytical application**

9 Under the optimized conditions, the calibration curve for determination of
10 formaldehyde was shown in Figure 5. With the increasing concentration of
11 formaldehyde, the R_{et} value increased correspondingly, implying a higher amount of
12 formaldehyde taken up the molecular recognition sites. $\Delta R/R$ was used as the
13 measurement signal, as it deciphered in Figure 5B, the measurement signal was
14 proportional to the logarithm of concentration of formaldehyde, ranging from 1
15 $\mu\text{mol}\cdot\text{L}^{-1}$ to 10 $\text{mmol}\cdot\text{L}^{-1}$. The detection limit was 0.8 $\mu\text{mol}\cdot\text{L}^{-1}$, which was lower
16 than previous reports, as shown in Table 1. So the electrospun nanofibers based
17 biomimetic hybrid film would emerge as a potential candidate for the biomimetic
18 recognition elements, showing great promise for the construction of nanoscale
19 biosensor.

20 The reproducibility of the resultant modified electrode before and after sensing
21 formaldehyde were evaluated, as shown in Fig 5C. The relative standard deviation
22 was calculated to be 6.6% and 2.5% estimated from the parallel response of five

1 different and freshly prepared electrode before and after immersing in $0.01 \text{ mol}\cdot\text{L}^{-1}$
2 formaldehyde-water solution, which revealed an excellent precision and acceptable
3 repeatability in the construction of the sensor.

4 To evaluate the selectivity of the fabricated biomimetic sensor, some compounds and
5 ions which could be possible interferences for formaldehyde liquid detection, were
6 used to examine the selectivity of the resultant biomimetic nanofibers based sensor, as
7 shown in the figure 5D. A foreign species was considered not to interfere if it caused
8 a relative error $<10\%$ for the measurement of $0.01 \text{ mmol}\cdot\text{L}^{-1}$ formaldehyde. The
9 results illustrated that the tolerated ratio of foreign substances to $0.01 \text{ mmol}\cdot\text{L}^{-1}$
10 formaldehyde was 50-fold for Cd^{2+} , Pb^{2+} , F^- , 100-fold for ethanol, methanol, carboxyl
11 contained acetone. To further explore effect of compounds with aldehyde group,
12 which could be potential interference in detection of formaldehyde, the acetaldehyde,
13 butyraldehyde were chosen to examine their performance of electrochemical
14 impedance spectroscopy. Then it was found that a little effect of acetaldehyde, but
15 neglectable interference of butyraldehyde existed in detection process of
16 formaldehyde, which indicated that the large activity of formaldehyde benefited to
17 this nucleophilic addition reaction, while larger steric effect and weaker nucleophile
18 would baffle this reaction⁴³. As a whole, the response signal after recognition of
19 formaldehyde was much larger than others'; which demonstrated the good selectivity
20 of this sensor. All the merits of the biomimetic recognition sensor based on
21 electrospun polymer nanofiber indicated that it might be sufficient for practical
22 applications.

1 **Conclusion**

2 In summary, this work elucidated a new biomimetic sensing interface for
3 formaldehyde based on electrochemical impedance spectroscopy. By combining
4 electrospinning method and molecularly imprinted hybrid, compared with the
5 traditional biomimetic materials, the proposed biomimetic nanofibers presented a
6 porous matrix with very large surface area to volume ration, much more binding sites,
7 and favorable binding characteristics, etc. Thus electrochemical impedance
8 spectroscopy was employed for the first time in monitoring the change resulted from
9 the target recognition took place at the binding sites on the surface of the nanofibers
10 by the target molecules. The prepared biomimetic sensor obtained a wide dynamic
11 response range with low limit of detection, ultra-sensitivity, satisfactory selectivity
12 and excellent reproducibility. This strategy was simple and specific, and it could be
13 coupled with other bio-recognition systems for other biological assays. Moreover, the
14 flexible sensing platform not only acted as the sensitized sensing element for
15 formaldehyde, but also offered a suitable carrier for immobilization of biomimetic
16 recognition elements on the surface of electrospinning nanofibers, which opens a
17 promising approach to develop further electrospun nanofibers to establish biomimetic
18 recognition sensor with favorable analytical performances.

19 **Acknowledged**

20 This project was financially supported by NSFC (21205016), National Science
21 Foundation of Fujian Province (2011J05020), Education Department of Fujian
22 Province (JA14071, JB14036, JA13068), Foundation of Fuzhou Science and

- 1
- 2
- 3
- 4 1 Technology Bureau (2013-S-113) and Fujian Normal University outstanding young
- 5
- 6 2 teacher research fund projects (fjsdjk2012068).
- 7
- 8
- 9 3
- 10
- 11
- 12
- 13
- 14
- 15
- 16
- 17
- 18
- 19
- 20
- 21
- 22
- 23
- 24
- 25
- 26
- 27
- 28
- 29
- 30
- 31
- 32
- 33
- 34
- 35
- 36
- 37
- 38
- 39
- 40
- 41
- 42
- 43
- 44
- 45
- 46
- 47
- 48
- 49
- 50
- 51
- 52
- 53
- 54
- 55
- 56
- 57
- 58
- 59
- 60

1
2
3
4 **References**
5

- 6
7 1. S. Bajwa, G. Mustafa, R. Samardzic, T. Wangchareansak and P. Lieberzeit,
8
9 Nanoscale Res. Lett., 2012, **7**, 328.
10
11 2. M. M.Ramon, S.Felix, B. Mustafa, H.Mandy , R.Knut and J. Mater. Chem., 2011,
12
13 **21**, 12588-12604.
14
15 3. M. E. Belowich and J. Fraser Stoddart., Chem. Soc. Rev., 2012, **41**, 2003-2024.
16
17 4. A. Hjelmencrantz and U. Berg, J. Org. Chem., 2002, **67**, 3585-3594.
18
19 5. S. Morales, F. G. Guijarro, J. L. G. Ruano and M. B. Cid, J. Am. Chem. Soc.,
20
21 2014, **136**, 1082-1089.
22
23 6. Z.Wang, H.Li, J.Chen, Z. Xue and B.Wu, X.Lu, Talanta, 2011, **85**, 1672-1679.
24
25 7. B.Rezaei and O.Rahmanian, Sens. Actuators B, 2011, **160**, 99-104.
26
27 8. C.Malitesta, I.Losito and P. G.Zambonin, Anal. Chem., 1999, **71**, 1366-1370.
28
29 9. H.Li, Z.Wang, B.Wu, X.Liu and Z.Xue, X.Lu, Electrochim. Acta, 2012, **62**,
30
31 319-326.
32
33 10. C.Xie, B.Liu, Z.Wang, D.Gao, G. Guan and Z.Zhang, Anal. Chem., 2008, **80**,
34
35 437-443.
36
37 11. J. Li, F. Jiang, Y.Li and Z.Chen, Biosens. Bioelectron., 2011, **26**, 2097-2101.
38
39 12. G. Z.Fang, J. Tan and X. P.Yan , Anal. Chem., 2005, **77**, 1734-1739.
40
41 13. B.M. Espinosa-García, W.M. Argüelles-Monal, J. Hernández, L. Félix-Valenzuela,
42
43 N. Acosta and F.M. Goycoolea, Biomacromolecules, 2008, **8**, 3355–3364.
44
45 14. X. Kan, Y. Zhao, Z.Geng, Z.Wang and J.J.Zhu, J. Phys. Chem. C, 2008, **112**,
46
47 4849-4854.
48
49
50
51
52
53
54
55
56
57
58
59
60

- 1
2
3
4 15. C. L.Choong, J. S.Bendall and W. I.Milne, *Biosens. Bioelectron.*, 2009, **25**,
5
6 652-656.
7
8
9 16. I. Chronakis, B.Milosevic, A.Frenot and L.Ye, *Macromolecules*, 2006, **39**,
10
11 357-361.
12
13
14 17. I.Chronakis, A.Jakob, B.Hagstrom and L.Ye, *Langmuir*, 2006, **22**, 8960-8965.
15
16
17 18. Y.Li, H.Yang, Q.You, Z.Zhuang and X. Wang, *Anal. Chem.*, 2006, **78**, 317-320.
18
19 19. X. Q. Wang, Y. Si, X. Mao, Y. Li, J. Y. Yu, H. P. Wang, B. Ding, *Analyst*, 2013,
20
21 **138**, 5129-5136.
22
23
24 20. B. Ding, X. F. Wang, J. Y. Yu, M. Wang, *J. Mater. Chem.*, 2011, **21**,
25
26 12784-12792.
27
28
29 21. M. S. Dresselhaus, G. Dresselhaus, P. C. Eklund, *Science of Fullerenes and Carbon*
30
31 *Nanotubes*, Academic Press: New York, 1996.
32
33
34 22. J. Li, A. Cassell, L. Delzeit, J. Han, M. Meyyappan, *J. Phys. Chem. B*, 2002, **106**,
35
36 9299-9305.
37
38
39 23. S.Mazinani, A.Ajji and C.Dubios, *J. Polym. Sci., Part B: Polym. Phys.*, 2010, **48**,
40
41 2052-2064.
42
43
44 24. H. R. Gerberich, G. C. Seaman, *Encyclopedia of Chemical Technology*, 1994,
45
46 929.
47
48
49 25. S. H. Wei, Y. J. Zhang, *Sensor Rev.*, 2014, **34**, 327-334.
50
51
52 26. W.Chan and T.Xie, *Anal. Chim. Acta.*, 1997, **339**, 173-178.
53
54
55 27. W.Vastarella and R.Nicastri, *Talanta*, 2005, **66**, 627-633.
56
57
58
59
60

- 1
2
3
4 1 28. M.Gonchar, M.Maidan, Y.Korpan , V.Sibirny, Z.Kotylak and A.Sibirny, FEMS
5
6 2 Yeast Res, 2002, **2**, 307-314.
7
8
9 3 29. K.Kawamura, K.Kerman, M.Fujihara, N.Nagatani, T.Hashiba and E.Tamiya, Sens.
10
11 4 Actuators B, 2005, **105**, 495-501.
12
13
14 5 30. L. P. Liu, X. G. Li, P.K.Dutta and J.Wang, Sens. Actuators B, 2013, **185**, 1-9.
15
16 6 31. M. Ben Ali, Y. Korpan, M. Gonchar, A. El'skaya, M. A. Maaref, N.
17
18 7 Jaffrezic-Renault and C. Martelet, Biosens. Bioelectron., 2006, **22**, 575-581.
19
20
21 8 32. T. Alizadeh and L. H. Soltani, J. Hazard. Mater., 2013, **248**, 401-406.
22
23
24 9 33. M. Yang, X. G. Zhang and H. L. Li, Analyst, 2001, **126**, 676-678.
25
26 10 34. Q. Y. Xing, W. W. Pei and R. Q. Xu, J. Pei, Basic Organic Chemistry, Higher
27
28 11 Education Press, Beijing, 2005.
29
30
31 12 35. Y.Gao, G.Sun, S.Wan and S.Zhu, Energy, 2010, **35**, 1455-1468.
32
33
34 13 36. X. Zhong, N. Bailey, K. Schesing S.Bian, L. Campos and A. Braunschweig., J.
35
36 14 Polym. Sci., Part B: Polym. Chem., 2013, **51**, 1533-1539.
37
38
39 15 37. J. Matsui, S.Goji, T. Murashima, D.Miyoshi, S.Komai, A.Shigeyasu, T.Kushida,
40
41 16 T.Miyazawa, T.Yamada, K.Tamaki and N. Sugimoto, Anal. Chem., 2007, **79**,
42
43 17 1749-1757.
44
45
46 18 38. Y. Zhang, M. Zhang, Z. Q. Cai, M. Q. Chen and F. L. Cheng, Electrochim. Acta,
47
48 19 2012, **68**, 172-177.
49
50
51 20 39. Y. N. Chen, X. H. Liu, W. Zhang, Y. Zhang, L. J. Li, Z. Z. Cao, H. Wang, G. Jia,
52
53 21 Y. F. Gao and J. R. Liu, Anal. Methods, 2013, **5**, 3915-3919.
54
55
56
57
58
59
60

- 1
2
3
4 40. L. T. Roman, M. A. Lomillo, D. R. Olga, M. S. César , M. A. Pilar and A. M.
5
6 Julia, Talanta, 2011, **86**, 324-328.
7
8
9 41. Z. L. Zhou, T.F. Kang, Y. Zhang and S.Y. Cheng, Microchim. Acta, 2009, **164**,
10
11 133-138.
12
13
14 42. A. Safavi, N. Maleki, F. Farjami and E. Farjami, J. Electroanal. Chem., 2009, **626**,
15
16 75-79.
17
18
19 43. S. Srinives, T. Sarkar, A. Mulchandani, Sens. Actuators, B 2014, **194**, 255-259.
20
21 8
22
23
24 9
25
26 10
27
28
29
30
31
32
33
34
35
36
37
38
39
40
41
42
43
44
45
46
47
48
49
50
51
52
53
54
55
56
57
58
59
60

1
2
3
4
5
6
7
8
9
10
11
12
13
14
15
16
17
18
19
20
21
22
23
24
25
26
27
28
29
30
31
32
33
34
35
36
37
38
39
40
41
42
43
44
45
46
47
48
49
50
51
52
53
54
55
56
57
58
59
60

1 **Table 1 Comparable figures of determining formaldehyde.**

Methods	Reagents	Linear ranges	LODs	Refs
Electrochemical sensor	Pd nanowires	0.002-1 mmol•L ⁻¹	0.5 μmol•L ⁻¹	38
Electroanalysis	Pt nanoparticles Graphene	0-2 mmol•L ⁻¹	40 μmol•L ⁻¹	39
Enzymatic sensor	alcohol oxidase	0.06-0.46 mmol•L ⁻¹	60 μmol•L ⁻¹	40
Electrochemical sensor	Pt-Pd nanoparticles	0.010-1 mmol•L ⁻¹	3 μmol•L ⁻¹	41
Electrocatalysis	Pd nanoparticles	20-100 mmol•L ⁻¹	10 mmol•L ⁻¹	42
Electrochemical impedance spectroscopy	CNTs@PAMH-nanofibers	0.001-100 mmol•L ⁻¹	0.8 μmol•L ⁻¹	This work

2

1 **Figure Legends**

2 **Scheme 1** Schematic routine of the biomimetic sensing platform for formaldehyde.

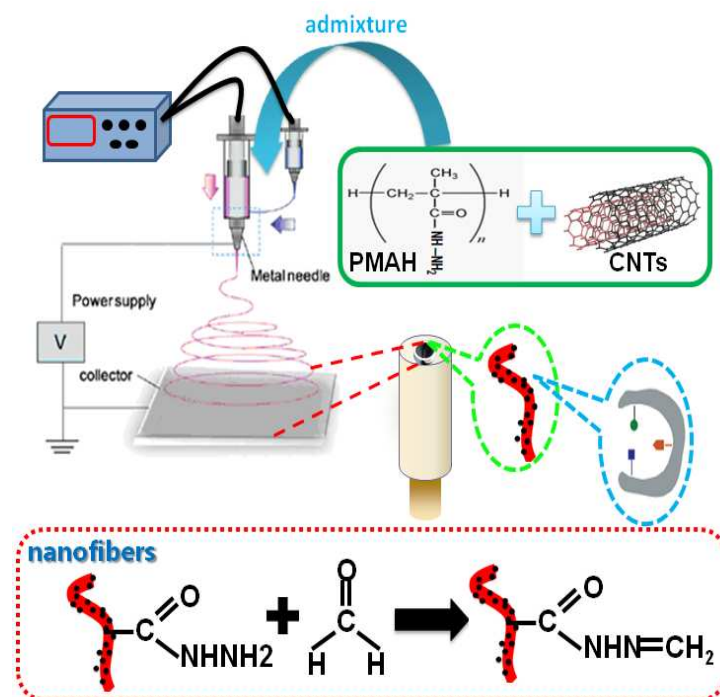
3 **Figure 1** (A) the SEM image of PMAH/CNTs-NFs, (B) the TEM image of
4 PMAH/CNTs-NFs, (C) FTIR spectra for (a) PMAH and (b) PMMA.

5 **Figure 2** (A) Cyclic voltammograms of various electrodes in $5 \text{ mmol}\cdot\text{L}^{-1} \text{ K}_3\text{Fe}(\text{CN})_6$
6 solution containing $0.1 \text{ mol}\cdot\text{L}^{-1} \text{ KCl}$. Scan rate: $100 \text{ mV}\cdot\text{s}^{-1}$. (B) Nyquist diagrams of
7 electrochemical impedance spectra of various electrodes. Electrolyte: $5 \text{ mmol}\cdot\text{L}^{-1}$
8 $[\text{Fe}(\text{CN})_6]^{3-/4-}$ and $0.1 \text{ mol}\cdot\text{L}^{-1} \text{ KCl}$. Bare GCE (a), PMAH/CNTs-NFs/GCE (b),
9 PMAH/CNTs-NFs/GCE incubated in $0.01 \text{ mol}\cdot\text{L}^{-1}$ formaldehyde solution for 60 s (c),
10 and PMAH-NFs/GCE (d).

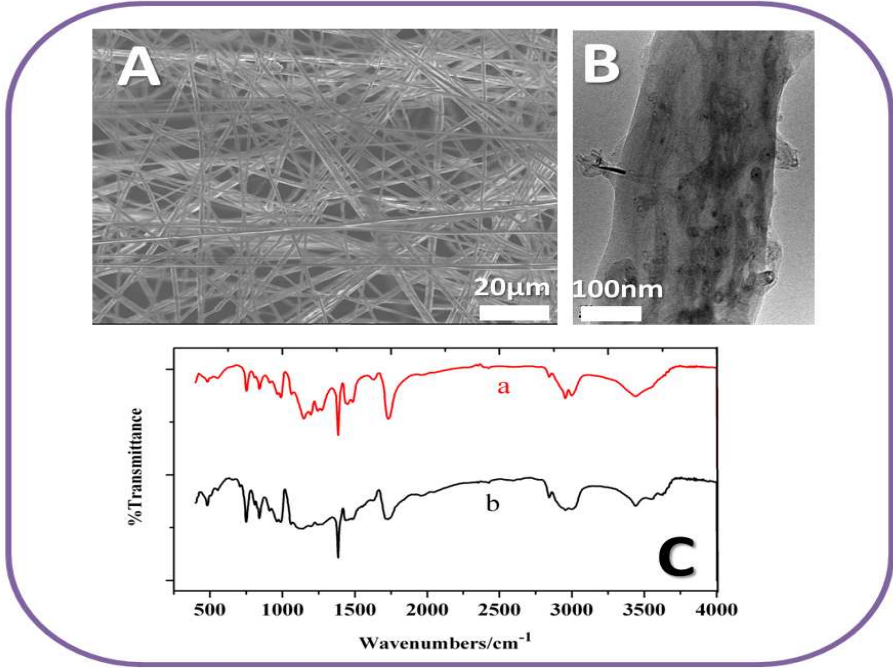
11 **Figure 3** (A) Nyquist diagrams of PMAH/CNTs-NFs/GCE (a),
12 PMAH/CNTs-NFs/GCE incubated in 0.01 M formaldehyde solution for 60 s (b),
13 PMAH-NFs/GCE (c), PMAH-NFs/GCE incubated in 0.01 M formaldehyde solution
14 for 60 s (d). (B) EIS of PMAH/CNTs/GCE (a), PMAH/CNTs-NFs/GCE (b),
15 PMAH/CNTs/GCE (c) and PMAH/CNTs-NFs/GCE incubated with $0.01 \text{ mol}\cdot\text{L}^{-1}$
16 formaldehyde solution for 60 s (d). Electrolyte: $5 \text{ mmol}\cdot\text{L}^{-1} [\text{Fe}(\text{CN})_6]^{3-/4-}$ and 0.1
17 $\text{mol}\cdot\text{L}^{-1} \text{ KCl}$.

18 **Figure 4** (A) Nyquist diagrams of electrochemical impedance spectra of (a)
19 PMMA-NFs/GCE and (b) PMMA-NFs/GCE incubated with $0.01 \text{ mol}\cdot\text{L}^{-1}$
20 formaldehyde solution for 60 s. (B) Effect of the amount of CNTs in the nanofibers on
21 the sensing performance for $0.01 \text{ mol}\cdot\text{L}^{-1}$ formaldehyde in $5 \text{ mmol}\cdot\text{L}^{-1} \text{ Fe}(\text{CN})_6^{3-/4-}$

1
2
3
4 1 solution containing $0.1 \text{ mol}\cdot\text{L}^{-1}$ KCl. (C) Effect of the amount of PMAH/CNTs-NFs
5
6 2 on the sensing performance of as-prepared sensor for $0.01 \text{ mol}\cdot\text{L}^{-1}$ formaldehyde . (D)
7
8 3 Impedance response for different times of preconcentration. Insert: impedance spectra
9
10 4 corresponding to the PMAH/CNTs-NFs/GCE electrode immersed in $0.01 \text{ mol}\cdot\text{L}^{-1}$
11
12 5 formaldehyde-water solution at different time (the time increased from a to e in turn).
13
14
15
16
17 6 **Figure 5** (A) Impedance spectrae of the PMAH/CNTs-NFs/GCE as the function of
18
19 7 formaldehyde concentration [(a) $1 \mu\text{mol}\cdot\text{L}^{-1}$, (b) $10 \mu\text{mol}\cdot\text{L}^{-1}$, (c) $50 \mu\text{mol}\cdot\text{L}^{-1}$, (d) 3
20
21 8 $\text{mmol}\cdot\text{L}^{-1}$, (e) $5 \text{ mmol}\cdot\text{L}^{-1}$, (f) $10 \text{ mmol}\cdot\text{L}^{-1}$] in $0.1 \text{ mol}\cdot\text{L}^{-1}$ KCl containing 5
22
23 9 $\text{mmol}\cdot\text{L}^{-1}$ $[\text{Fe}(\text{CN})_6]^{3-/4-}$. (B) Calibration curve for the electrospon sensor. (C)
24
25 10 Impedance spectra for $5 \text{ mmol}\cdot\text{L}^{-1}$ $[\text{Fe}(\text{CN})_6]^{3-/4-}$ solution containing $0.1 \text{ mol}\cdot\text{L}^{-1}$ KCl
26
27 11 at PMAH/CNTs-NFs/GCE before (a) and after immersing into $0.01 \text{ mol}\cdot\text{L}^{-1}$
28
29 12 formaldehyde solution for 60 s (b). (D) Selectivity of PMAH/CNT-NFs/GCE for 0.01
30
31 13 $\text{mol}\cdot\text{L}^{-1}$ formaldehyde, $0.5 \text{ mol}\cdot\text{L}^{-1}$ F^- , Cd^{2+} , Pb^{2+} and $1 \text{ mol}\cdot\text{L}^{-1}$ methanol, ethanol,
32
33 14 acetone, butyraldehyde, acetaldehyde.
34
35
36
37
38
39
40
41
42
43
44
45
46
47
48
49
50
51
52
53
54
55
56
57
58
59
60



Scheme 1



1

2

3

4

Figure 1

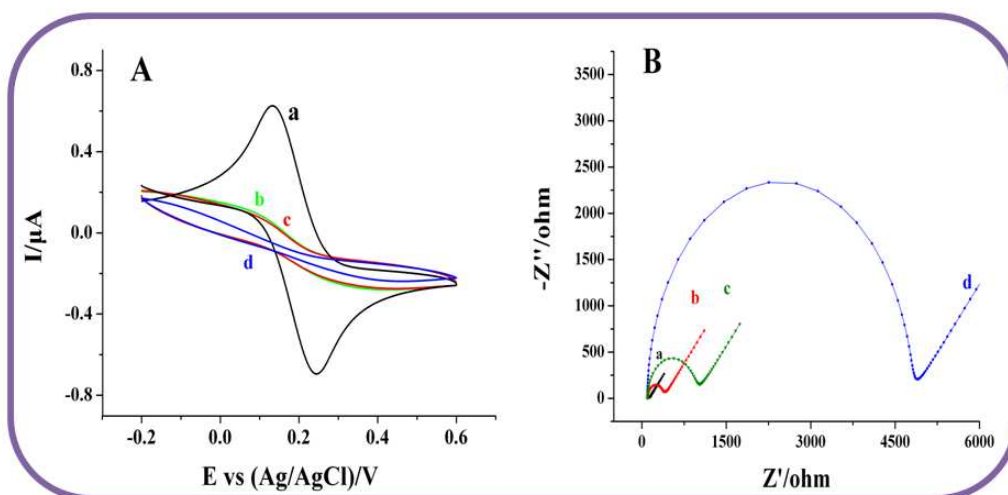
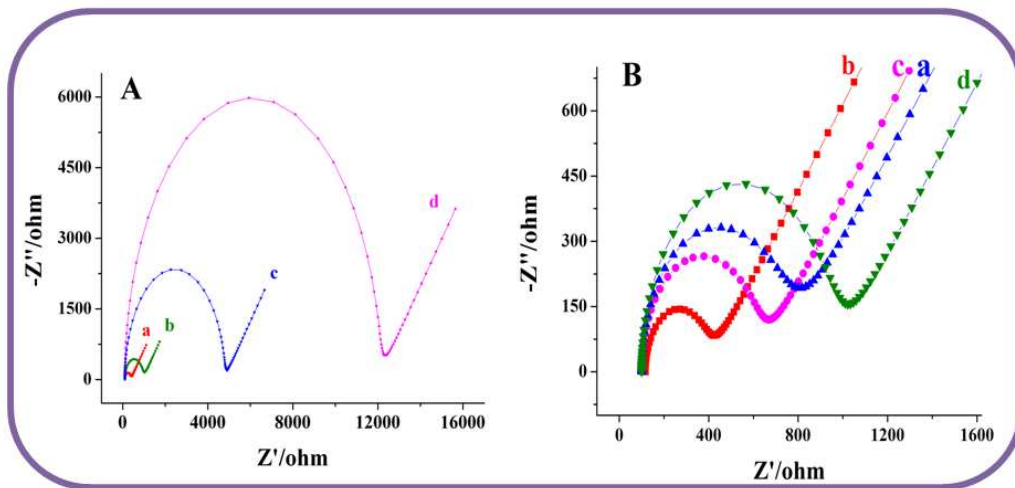


Figure 2

1
2
3
4
5
6
7
8
9
10
11
12
13
14
15
16
17
18
19
20
21
22
23
24
25
26
27
28
29
30
31
32
33
34
35
36
37
38
39
40
41
42
43
44
45
46
47
48
49
50
51
52
53
54
55
56
57
58
59
60



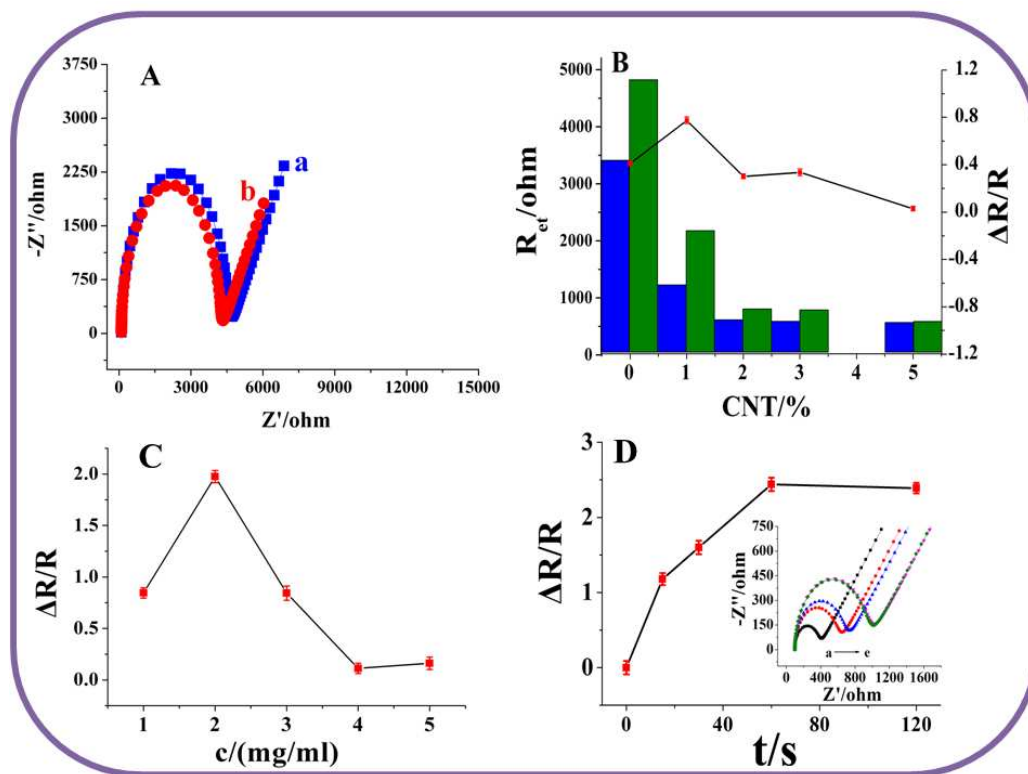
1

2

3

4

Figure 3



1

2

3

4

Figure 4

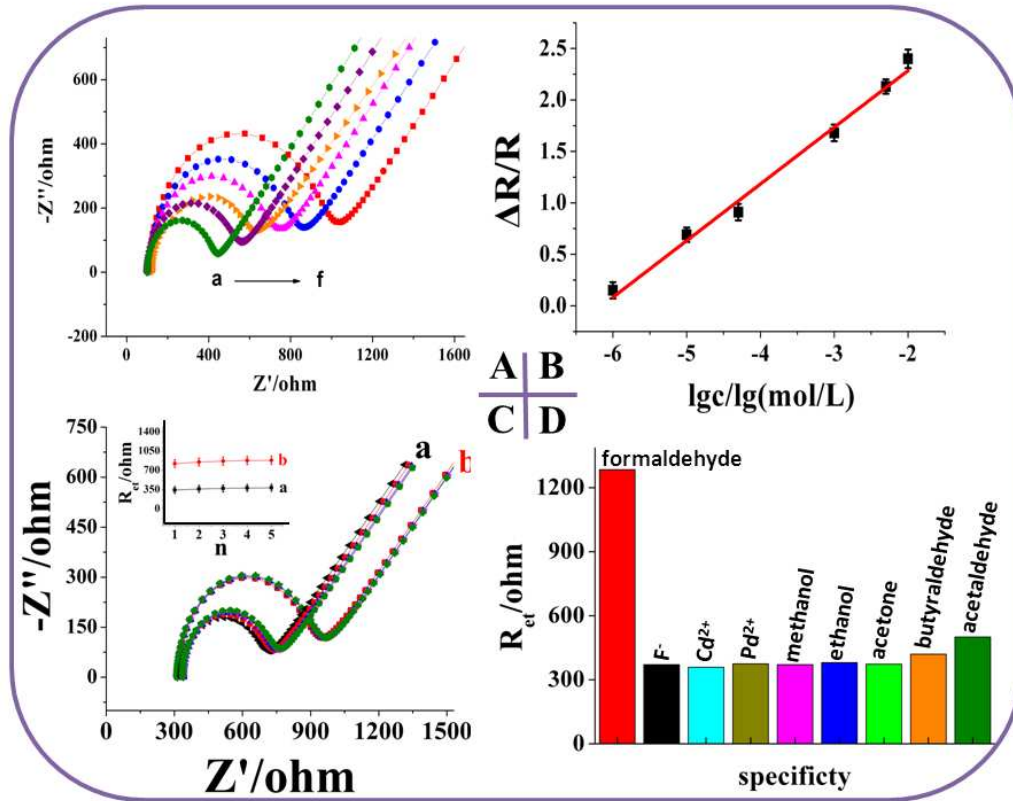


Figure 5

